

Review

Evidence for Helical Magnetic Fields Associated with AGN Jets and the Action of a Cosmic Battery

Denise Gabuzda

Physics Department, University College Cork, Cork T12 K8AF, Ireland; d.gabuzda@ucc.ie; Tel.: +353-21-490-2003

Received: 9 November 2018; Accepted: 14 December 2018; Published: 27 December 2018



Abstract: Theoretical models for the electromagnetic launching of astrophysical jets have long indicated that this process should generate helical magnetic fields, which should then propagate outward with the jet plasma. Polarization observations of jets are key for testing this idea, since they provide direct information about the magnetic field structures in the synchrotron-emitting radio jets. Together with Faraday rotation measurements, it is possible in some cases to reconstruct the three-dimensional magnetic-field structure. There is now plentiful evidence for the presence of helical magnetic fields associated with the jets of active galactic nuclei, most directly the detection of transverse Faraday-rotation gradients indicating a systematic change in the line-of-sight magnetic field component across the jets. A variety of models involving helical jet magnetic fields have also been used to explain a great diversity of phenomena, including not only the linear polarization and Faraday rotation structures, but also circular polarization, anomalous wavelength dependences of the linear polarization, variability of jet ridge lines, variability of the Faraday rotation sign and polarization angle rotations. A joint consideration of Faraday rotation measurements on parsec and kiloparsec scales indicates a magnetic-field and current structure similar to that of a co-axial cable, suggesting the action of some kind of battery mechanism, such as the Poynting–Robertson cosmic battery.

Keywords: active galactic nuclei; relativistic jets; magnetic fields; radio interferometry

1. Introduction

In normal galaxies such as our Milky Way, the vast majority of the luminosity is associated with thermal emission from stars and glowing gas. Although virtually all galaxies are believed to harbour a supermassive black hole in their central regions, with masses of order 10^6 solar masses, the emission associated with accretion onto this central black hole comprises a small fraction of the overall luminosity of the galaxy. However, the luminosities of a minority of galaxies are dominated by the contribution of non-thermal activity in their nuclei. The strongest of such Active Galactic Nuclei (AGN) are about 10^5 -times more luminous than a normal galaxy such as the Milky Way. The activity giving rise to this tremendous energy is believed to be accretion onto a much more massive supermassive black hole ($\sim 10^9$ solar masses) at the galactic centre.

This accretion process sometimes, but not always, creates conditions favourable for the generation and launching of jets of relativistic plasma from the vicinity of the central black hole in the AGN. Although no direct imaging is available, it is natural to suppose that these jets are ejected along the rotational axis of the central black hole. The relativistic electrons present in these jets and the lobes they inflate at their termination points emit radio synchrotron radiation as they move through regions with magnetic (**B**) fields. About 10–15% or so of all AGN, said to be “radio-loud”, display substantial amounts of such radio emission (ratio of the 5-GHz flux to the optical B-band flux ≥ 10 [1]). The presence of synchrotron radiation requires both highly relativistic particles and magnetic fields,

suggesting that the jets are regions where particle acceleration and magnetic-field amplification can occur.

The jet launching mechanism is widely believed to be electromagnetic in nature. In the Blandford–Payne process [2], a magnetic (\mathbf{B}) field threading the accretion disk and frozen into the disk plasma is wound up by the rotation of the disk. This gives rise to a magnetic pressure gradient that accelerates material from the disk outward along the field lines. The Blandford–Znajek mechanism [3] provides a means of extracting the rotational energy of the black hole. The rotation of the black hole in the ambient \mathbf{B} field from the accretion disk gives rise to induced electric fields that accelerate local charged particles, initiating a series of processes that gives rise to jets comprised of electrons and positrons carried outward by an outgoing Poynting flux. A key factor in both mechanisms is rotation of the central black hole and its accretion disk in the presence of a magnetic field, giving rise to a helical \mathbf{B} field carried outward along with the jets. The generation of such fields has been investigated theoretically in a number of studies over the years. Two of the best-known earlier works in this area are those of Nakamura et al. [4] and Lovelace et al. [5]. Some of the most recent simulations of jet launching and propagation have been done, for example, by Tchekhovskoy and Bromberg [6] and Barniol Duran et al. [7]; many more examples can be found in the literature. The azimuthal/toroidal component of this helical field may well also play a role in collimating the jets. The magnetic field threading the accretion disk is often taken to be more or less randomly oriented, but it has a preferred orientation in some scenarios, such as the “cosmic battery” model described by Contopoulos et al. [8] and Christodoulou et al. [9]. Furthermore, the presence of a toroidal field component unambiguously implies the presence of a current in the jet, whose direction is given by the usual right-hand rule from university physics (Figure 1, adapted from [10]); thus, studies of helical fields associated with AGN jets are intrinsically tied to studies of the currents flowing in AGN jets.

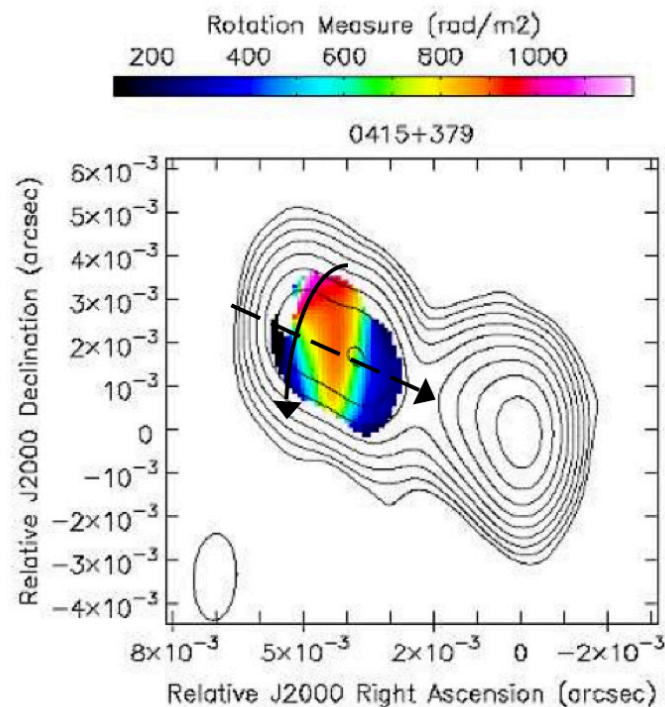


Figure 1. Relationship between an observed transverse Faraday RM gradient (colour scale), the direction of the associated azimuthal \mathbf{B} field component (solid curved arrow) and the inferred direction of the current, inward in this case (dashed arrow). RM image superposed on intensity contours adapted from [10].

One of the signatures of synchrotron radiation is significant linear polarization. Synchrotron radiation can, in principle, be completely unpolarized if the synchrotron \mathbf{B} field is fully disordered; if the magnetic field is partially or fully ordered, however, this will lead to a corresponding degree of linear polarization, up to a maximum of about 75% for a fully-ordered magnetic field and a random pitch angle distribution for the population of radiating electrons [11]. The direction of the observed plane of linear polarization will be orthogonal to the synchrotron magnetic field in the case of optically-thin emission. The plane of linear polarization becomes aligned with the synchrotron \mathbf{B} field in sufficiently optically-thick regions; however, this transition actually occurs at an optical depth considerably exceeding unity [12]. This means that the polarized emission we observe in radio images of AGN jets is likely all predominantly from optically-thin regions, including polarization from the “core”, often interpreted as the location along the jet outflow where the optical depth is near unity [13].

Linear-polarization observations are the only source of direct information about both the orientation of the synchrotron \mathbf{B} field and the extent to which this field is ordered. For this reason, polarization observations play a key role in studies of both AGN jets and the media through which they propagate. They are also an important means of searching for evidence of the helical \mathbf{B} fields predicted to form during the launching of the jets.

Very Long Baseline Interferometry (VLBI) provides a means of imaging AGN with very high resolution, in order to obtain information about regions that are as close as possible to the “central engine” and jet-launching region. The jets of AGN are present on the smallest scales it has been possible to directly image with VLBI. At the other end, they can extend many kiloparsecs from the galactic nucleus, often displaying extremely good collimation. Observations of high resolution at multiple wavelengths are required if we wish to obtain information about the spectrum of the radio emission and Faraday rotation of the polarization angles arising at various locations between the emission region and the observer. The detection of a systematic Faraday-rotation gradient across an AGN jet can reveal the presence of a toroidal \mathbf{B} -field component in the immediate vicinity of the jet, possibly associated with the helical \mathbf{B} field predicted to form when the jets are launched (see Section 2.2).

In addition to the helical \mathbf{B} fields that should be carried outward with the jets, there are numerous local phenomena that can also considerably influence the observed jet \mathbf{B} fields, such as shocks, interactions with the surrounding medium, bending of the jets, turbulence and magnetic reconnection. Thus, one of the observational challenges is to determine which features are mainly associated with the action of local effects and which are mainly a consequence of the intrinsic helical/toroidal magnetic fields of the jets.

2. Observational Evidence for Helical \mathbf{B} Fields in AGN Jets

2.1. Linear Polarization Structures

Variety of Observed Structures

The observed polarization in the jets of AGN on parsec scales usually tends to lie either parallel to or perpendicular to the local jet direction, with the inferred direction of the associated jet \mathbf{B} field being orthogonal to the direction of the polarization, assuming the polarized emission arrives from predominantly optically-thin regions [14]. We should note here that the 90° rotation in the orientation of the observed linear polarization from orthogonal to aligned with the synchrotron \mathbf{B} field in the transition from optically thin to optically thick occurs at an optical depth τ substantially greater than unity ($\tau \simeq 6$ [12]), so that even polarization observed in the VLBI core region (optical depth $\simeq 1$) is expected to arise in predominantly optically-thin regions. Thus, the assumption that the observed polarization patterns are associated with optically-thin emission is well justified.

Commonly-observed polarization patterns correspond to: (a) extensive regions of \mathbf{B} field aligned with the local jet direction; (b) localized regions of \mathbf{B} field oriented perpendicular to the local jet direction, associated with bright, compact features; (c) extensive regions of \mathbf{B} field oriented perpendicular to the local jet direction; (d) the spine-sheath \mathbf{B} -field structure across the jet; (e) \mathbf{B}

field aligned with the local jet direction and offset toward one side of the jet; and (f) **B** field aligned with the local jet direction around the outer edge of a bend in the jet. For brevity, we will refer to **B** field (or polarization) aligned with the jet as “longitudinal” and **B** field (or polarization) perpendicular to the jet as “orthogonal.” A schematic of these various polarization configurations is shown by Gabuzda [15]. Lyutikov et al. [16], for example, have pointed out that this could be a natural consequence of local cylindrical symmetry displayed by the jets; in this case, the **B** field can always be described as a sum of longitudinal and orthogonal components projected onto the sky.

In fact, helical jet **B** fields could give rise to virtually all of these characteristic polarization patterns, as outlined below.

- (a), (c) Extended regions of longitudinal or orthogonal **B** field could be associated with helical jet **B** fields with comparatively low and high pitch angles (i.e., comparatively “loosely-wound” or “tightly- wound” helical fields), respectively. The pitch angle of the helical field should be due in part to the ratio of the velocities of the rotation and outflow.
- (d) A spine-sheath transverse polarization structure refers to a situation in which the predominant **B** field is orthogonal near the jet axis and longitudinal at one or both edges of the jet. This configuration could be associated with an overall helical field, with the azimuthal component of the field dominant near the jet axis, where its projection is orthogonal to the jet, and the longitudinal component of the helical field dominant near the jet edges, where its projection is along the jet (e.g., [16,17]). In this case, we would also expect to observe an increase in the degree of polarization from the central axis toward the jet edges.
- (e) Depending on the pitch angle of the helical field and the viewing angle of the jet, situations are possible in which the longitudinal **B** field predominates on one side of the jet, while the orthogonal **B** is dominant on the other. If the orthogonal **B** field is too weak to be detected in a particular image, this may also appear as a region of the longitudinal **B** field offset toward one side of the jet on its own (see, e.g., [18]).
- (f) The well-ordered longitudinal **B** field around the outer part of a bend in the jet could come about when the longitudinal component of a helical **B** field is enhanced by the curvature of the jet, stretching the **B** field at the outer edge of the bend.

The only type of pattern that is not naturally explained by the presence of helical jet **B** fields is regions of the orthogonal **B** field associated with bright, compact regions, which are probably more naturally associated with shock compression (see, e.g., [19–22]).

Most of these polarization patterns can also be caused by combinations of other, locally-acting, phenomena, such as interactions with the ambient medium. However, the principle of Occam’s razor is relevant here, which can be stated as “if more than one explanation is possible, the simplest should be preferred”. Another way of expressing this principle is that, the more assumptions that must be made to explain observations, the more unlikely the explanation. Since helical jet **B** fields are predicted theoretically to be present, Occam’s razor suggests an approach in which we initially ask which of the observed polarization characteristics can straightforwardly be explained by the jet’s helical field; if all the observed characteristics can be explained by this one theoretically-based assumption, this provides the simplest explanation of the observations. We can then look to other factors such as superposed shocks and shear to explain localized, anomalous or unusual features not easily explained by a helical jet **B** field, guided by additional information, such as variability or spectral data when possible. This approach is most likely to provide a relatively complete picture of the jet itself and the actions of various agents on it as it propagates outward from the AGN.

Another interesting question is whether the jet fluid itself follows helical stream lines, as in the picture of [23], or possibly even rotates as it propagates from the jet base, and what effect this may have on the observed polarization patterns in the jets. Marscher et al. [24] have suggested that one observational manifestation of motion of the jet plasma along helical stream lines could be rapid and smooth rotations of the observed polarization angles, probably upstream of the VLBI core. More

direct evidence for the existence of streamline-like structures comes from the detection of oscillatory intensity structures within the overall jet flow in a few well-resolved AGN jets (e.g., [25,26]). However, at present, we have no firm information about how the presence of such helical streamlines in the VLBI jets could potentially affect the observed polarization, although this question is worthy of further study. In terms of possible rotation of the jet plasma, we have no means of detecting this directly, and no indirect evidence for rotation of AGN jets has been reported thus far, making it premature to speculate about possible effects of such rotation on the observed polarization patterns at this time.

It is also of interest to consider how the above polarization patterns could be affected by the angle at which a jet carrying a helical \mathbf{B} field is viewed. This has been analysed, for example, by Murphy et al. [18], who presented figures summarizing the types of polarization structure observed for various combinations of helical pitch angle and viewing angle (Figures 1 and 2 of [18]). For example, taking into account the typical resolution of centimetre-wavelength VLBI observations, a jet carrying a helical field with a pitch angle in the rest frame of the jet of 80° will display the transverse \mathbf{B} field all across the jet when the viewing angle in the rest frame of the jet is $80\text{--}90^\circ$, the longitudinal \mathbf{B} field on one side and the transverse \mathbf{B} field on the other if this viewing angle is roughly $60\text{--}80^\circ$ and the longitudinal \mathbf{B} field at the edges and the transverse \mathbf{B} field near the jet axis (a “spine + sheath” structure) if this viewing angle is less than about 60° . A technique for deriving the intrinsic speed of the jet and the viewing angle in the observer’s frame from (i) the pitch angle of the helical \mathbf{B} field and the viewing angle in the rest frame of the jet derived from fitting transverse intensity and polarization profiles and (ii) the observed superluminal speeds in the jet is described in [18].

2.2. Faraday Rotation Gradients

An electromagnetic wave can be described as the sum of any two mutually-perpendicular components of the wave’s electric field. In radio astronomy, these are often taken to be the Right Circularly-Polarized (RCP) and Left Circularly-Polarized (LCP) components of the \mathbf{E} field. When such a wave passes through a magnetized medium present along the path from the source to the observer, asymmetry in the interactions between free electrons in the medium and the RCP and LCP components of the polarized electromagnetic wave leads to these two components having different speeds of propagation in the medium. This means that the RCP and LCP components become more and more out of phase as the wave passes through the medium, manifest as a rotation of the plane of polarization of the wave, known as Faraday rotation. The amount of rotation depends on the strength of the ambient magnetic field \mathbf{B} , the number density of charges in the plasma n , the charge e and mass m of these charges and the wavelength of the radiation λ :

$$\chi = \chi_o + \text{RM}\lambda^2 \quad \text{RM} = \frac{e^3}{8\pi^2\epsilon_o m^2 c^3} \int n\mathbf{B} \cdot d\mathbf{l} \quad (1)$$

where χ is the observed and χ_o the intrinsic emitted polarization angle, RM the Faraday Rotation Measure, ϵ_o the permittivity of free space and c the speed of light in a vacuum, and the integral is carried out over the line of sight from the source to the observer.

Although Faraday rotation can, in principle, be associated with any free charged particles in the magnetized plasma in which it arises, due to the $1/m^2$ dependence in the expression for the RM, it is usually assumed that the observed RM is due to electrons, rather than protons. Furthermore, because relativistic electrons have appreciably higher effective masses than non-relativistic ones, the electrons giving rise to the Faraday rotation are usually assumed to be non-relativistic (thermal). The RM depends on both the electron density and the Line Of Sight (LOS) \mathbf{B} field; however, the sign of the RM is determined purely by whether the LOS \mathbf{B} field is pointed toward (positive) or away from (negative) the observer. This means that the sign of the RM provides a unique diagnostic of the structure of the associated \mathbf{B} field along the line of sight. In the simplest case when the Faraday rotation occurs outside the emitting volume in the source, it gives rise to a linear dependence of χ on λ^2 , as is indicated above, providing a straightforward means of identifying the action of Faraday rotation observationally.

If a jet and its immediate vicinity carry a helical \mathbf{B} field, this will give rise to a monotonic gradient in the observed Faraday rotation across the jet, due to the monotonic change in the LOS component of the helical \mathbf{B} field across the jet. Some observers and theoreticians were aware of this effect as long ago as the 1980s (e.g., [27,28]), but it was largely ignored until the detection of a Faraday-rotation gradient across the parsec-scale jet of 3C273, reported in 2002 by Asada et al. [29].

Transverse RM gradients with statistical significances exceeding the 3σ level have now been detected across the jets of about 50 AGNs [30] and also across the kiloparsec-scale jet structures of a number of AGNs and radio galaxies [9,31]). The overall patterns displayed by these transverse RM gradients are discussed in the following subsection.

Note that, in principle, an RM gradient across a jet could come about due to a corresponding gradient in the electron density in a Faraday screen in the vicinity of the jet. However, variations in the electron density in the region of Faraday rotation cannot cause changes in the sign of the RM, whereas a transverse RM gradient due to a helical jet \mathbf{B} field can encompass RM values of both signs. It is therefore noteworthy that an appreciable number of the transverse RM gradients detected across AGN jets change sign across the jet. Note also that, depending on the pitch angle of the helical field and the jet viewing angle, an RM gradient due to a helical jet \mathbf{B} field may include RM values of only one sign, so that the lack of a sign change across the jet is not an argument against interpreting an RM gradient as reflecting the presence of a helical magnetic field being carried by the jet.

2.2.1. Overall Patterns of the Transverse RM Gradients on pc and kpc Scales: Evidence for the Action of a Cosmic Battery

The direction of an RM gradient observed across the jet of an AGN implies a direction for the azimuthal (toroidal) magnetic-field component that is giving rise to this gradient, which, in turn, implies the direction for a current associated with this toroidal field (Figure 1). The direction of the azimuthal component of the jet's helical field basically comes about due to the combination of the direction of the rotation of the central black hole and its accretion disk and the direction of the longitudinal field component that is partially transformed into a toroidal component by the rotation.

In this simplest picture, we would expect to see a particular direction for the observed transverse RM gradient all along the jet. This is true in some cases; in addition, transverse RM gradients in the same direction have been observed at multiple epochs in some AGN, indicating that these structures are fairly stable. However, at the same time, reversals in the directions of observed transverse RM gradients have been observed in a number of cases, either with distance from the base of the jet or with time (see [30] and references therein). This can be understood as a consequence of a structure with nested helical fields surrounding the jet, one inside the other, with the directions of the azimuthal field components being opposite in the two [32]. In this case, the line of sight passes through both regions of the helical \mathbf{B} field, and the direction of the net observed RM gradient is determined by which region (inner or outer) makes the greater contribution to the overall Faraday rotation. If conditions in and around the jet lead to a change in whether the inner or outer region of helical field dominates the observed Faraday rotation, this will lead to a corresponding change in the direction of the associated RM gradient across the jet.

In fact, just such a nested helical-field configuration is expected in the “cosmic battery” model of [8,9]. Further, this model predicts that the orientations of the azimuthal components of the two regions of helical field are not random: the inner helical field should have a counter-clockwise azimuthal component projected onto the sky, associated with an inward current along the jet (as in the example shown in Figure 1), while the outer helical field should have a clockwise azimuthal component projected onto the sky, associated with a more extended region of outward current (essentially present between the two regions of the helical field). This situation is shown schematically in Figure 2.

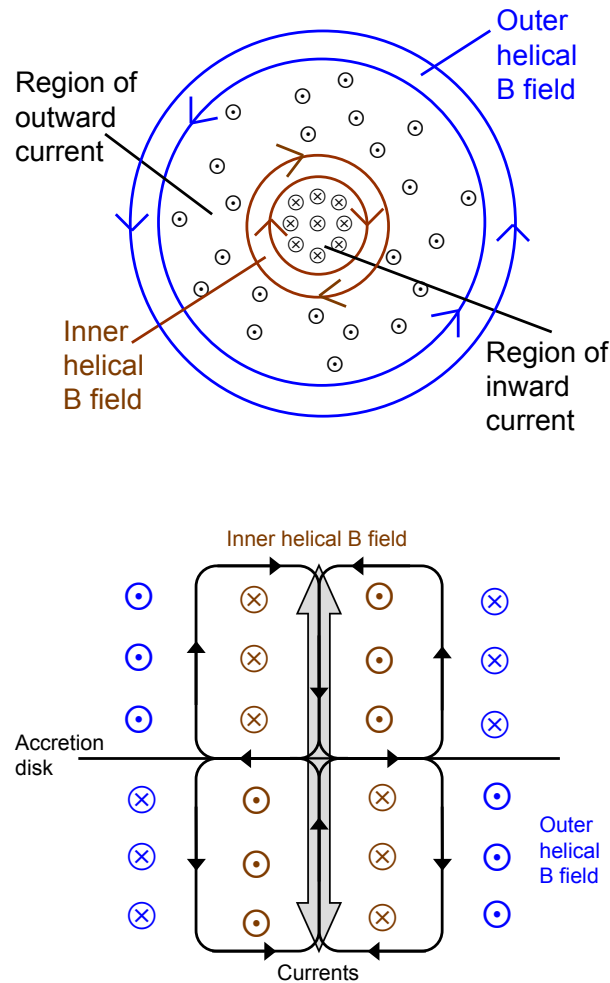


Figure 2. Schematic views of the set of helical \mathbf{B} fields and associated currents inferred from parsec-scale and kiloparsec-scale Faraday RM gradients looking straight down the jet axis (upper) and viewed at 90° to this, in the plane of the accretion disk (lower). The overall configuration of currents resembles a coaxial cable, with inward current along the jet axis and a more extended region of outward current farther from the axis.

Sufficient statistics to test this picture have recently become available. Gabuzda et al. [30] have demonstrated that the collected data on RM gradients detected across about 50 AGN jets imaged with centimetre-wavelength VLBI indicate a statistically-significant predominance of inward currents (probability of the predominance being spurious $\simeq 0.40\%$). In contrast, the results of [9], supplemented by the more recent results of [31], show the opposite tendency: a strong predominance of outward currents on decaparsec–kiloparsec scales (probability of the predominance being spurious $\simeq 0.05\%$). These observations are consistent with a picture in which the jets have a nested helical-field configuration, with huge current loops oriented roughly orthogonal to the accretion disk, with the current flowing inward along the jet axis, away from the axis in the accretion disk, outward in an extended region around the jet and back toward the jet axis in a region near the termination of the jet. Determining the physical origin and nature of this set of \mathbf{B} fields and currents will provide key information for our understanding of the formation and propagation of AGN jets.

This is broadly similar to the set of currents and \mathbf{B} fields in a co-axial cable, but extending over kiloparsec scales. It is important that the data suggest not only a nested helical-field configuration, but specifically one corresponding to inward current along the jet axis and outward current in a more

extended region around the jet. It is this clear preference for a particular direction for the currents flowing in and around the jets that strongly suggests the action of some kind of battery, such as the mechanism of [8,9]. Of course, other competing mechanisms may come to light; however, at present, this is the only mechanism specifically predicted to give rise to this configuration of fields and currents.

As was pointed out in [30], it is also interesting that a sizeable minority of the transverse RM gradients that have been detected on parsec scales correspond instead to outward currents. It may be that, in these sources, the outer region of the helical field has already become dominant on scales smaller than those on which the gradient is detected. It may also be that the battery-like mechanism that is leading to a dominance of inward currents along the jet axis on parsec scales is less efficient under some conditions; in this case, a relatively small number of the observed transverse RM gradients could have random directions. One of the most intriguing possibilities is that the cosmic battery mechanism described above may operate in the opposite sense (“in reverse”) when the central black hole rotates very rapidly, at more than about 70% of its maximum possible rotational velocity, as suggested by the numerical computations of [33]. The inner edge of the accretion disk will approach closer to the black hole event horizon as the rotational velocity increases. If the rotation is fast enough, the inner edge of the disk is located close enough to the horizon for the rotation of space-time to exert the dominant effect, rather than the disk’s rotation. This leads to a reversal in the direction of the radiation force on the electrons in the accretion disk, so that electrons acquire higher, rather than lower, toroidal velocities in the direction of rotation compared to protons in the disk. Searches for differences in the properties of AGNs whose transverse RM gradients correspond to predominant inward and outward currents in their jets on parsec scales would be valuable in this context.

2.2.2. Helical vs. Toroidal Fields

The detection of a transverse RM gradient indicates the presence of an azimuthal **B**-field component, but, on its own, this does not demonstrate that this is one component of an overall helical **B** field. It is therefore important to identify observational diagnostics that can distinguish whether this azimuthal field represents a toroidal field or one component of a helical **B** field. The key to this is whether the intensity and polarization profiles across the jet are symmetric or asymmetric. A toroidal field has no net longitudinal component (because this component is either absent or disordered) and will give rise to symmetric intensity and polarisation profiles across the jet, whereas a helical field has an ordered longitudinal component, which will give rise to asymmetric profiles across the jet. The key point here is that the synchrotron intensity and degree of polarization are both determined by the **B** field component in the plane of the sky.

When helical and toroidal fields are viewed side-on, it becomes apparent that a toroidal field will generally appear symmetric about the central jet axis, whereas a helical field will display asymmetry if viewed at any angle other than exactly 90° to the jet axis (Figure 3). A toroidal field should give rise to symmetric intensity and polarization profiles, independent of the angle at which the jet is viewed. However, the presence of a longitudinal component in the helical field introduces asymmetry. The dominant **B** field along one edge of the jet (top edge of the lower helical field in Figure 3) lies close to the line of sight, and we observe relatively lower degrees of polarization; in contrast, the dominant **B** field along the other edge of the jet (bottom edge of the lower helical field in Figure 3) lies close to the plane of the sky, and we observe relatively higher degrees of polarization. Only for particular viewing angles and helical pitch angles will a helical **B** field give rise to symmetrical intensity and polarization structures (see, e.g., [18,30]).

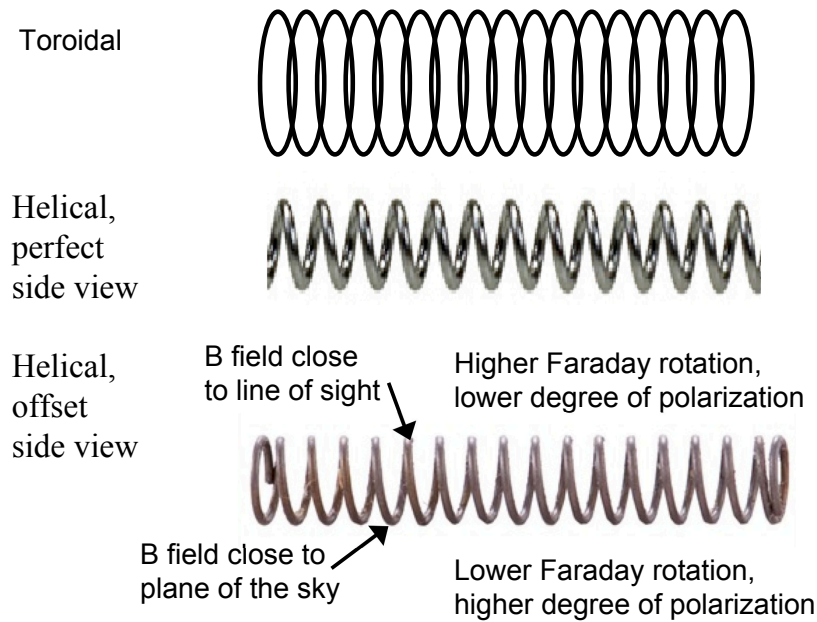


Figure 3. Schematic showing differences in the profiles presented by a toroidal field (upper image), a helical field viewed exactly side-on (middle image) and a helical field viewed slightly offset from exactly side-on (lower image). The jet axes are horizontal in each case and run down the centres of the toroidal and helical configurations shown. The first two cases give rise to symmetrical polarization profiles, whereas the last case gives rise to asymmetrical polarization profiles (in observations with sufficient resolution to detect this effect). In the offset side-view shown for the lower helix, the \mathbf{B} field is oriented close to the line of sight along the upper edge of the helix and closer to the plane of the sky at the lower edge of the helix. Because Faraday rotation is proportional to the LOS \mathbf{B} field, we expect the magnitude of the Faraday rotation to be higher at the upper than at the lower edge of this jet. Because the degree of polarization of synchrotron radiation is determined by the \mathbf{B} field in the plane of the sky (perpendicular to the line of sight toward the observer), we expect the degree of polarization to be higher at the lower than at the upper edge of this jet.

In addition, the fact that Faraday rotation is proportional to the LOS component of the ambient \mathbf{B} field provides additional potential tests of consistency of observations with the presence of helical \mathbf{B} fields in jets displaying transverse Faraday RM gradients. The picture depicted in Figure 3 predicts that the side of such a jet with the higher degree of polarization (dominant \mathbf{B} -field component in the plane of the sky) should display a lower amount of Faraday rotation, whereas the side of the jet with the lower degree of polarization (dominant \mathbf{B} -field component along the line of sight) should display a higher amount of Faraday rotation. Indeed, some cases where this pattern is observed have been noted [18], but much more work remains to be done.

We should note that it may seem at first inappropriate to speak of viewing a helical field side-on, as in Figure 3), since we believe the jets of core-dominated AGN are oriented close to our line of sight. However, taking into account aberration, a small viewing angle of close to $1/\Gamma$ in the observer's frame (where Γ is the Lorentz factor for the bulk relativistic motion of the jet) will be close to a viewing angle of 90° in the jet rest frame, corresponding to the situations shown in Figure 3).

2.3. Variability of the Faraday Rotation Sign

During their monthly monitoring of the AGN Mrk421 at 15, 24 and 43 GHz with the Very Long Baseline Array in 2011, Lico et al. [34] discovered time variability in both the magnitude and the sign of the Faraday RM in the core region. Since the RM sign is determined by the direction of the LOS \mathbf{B} field,

it is not trivial to explain such rapid changes in the RM sign. They suggest that the RM sign reversals observed during their monitoring can be understood if the jet has a nested helical-field configuration such as the one described in Section 2.2.1 and depicted in Figure 2, with opposite directions for the azimuthal field components in the inner and outer regions of the helical \mathbf{B} field; in this case, the variability of the RM sign could come about due to changes in whether the inner or outer region of the helical field dominates the observed Faraday rotation.

In fact, although the RM signs observed for some AGN can be stable over many years, the RM sign is variable for others. Furthermore, changes in the RM sign are also sometimes observed along the core-jet structure, even after taking into account the Faraday rotation occurring in our own galaxy. Such sign changes reflect changes in the direction of the LOS \mathbf{B} field relative to our line of sight and so provide information about the three-dimensional \mathbf{B} fields of these jets. The suggestion of Lico et al. [34] that RM sign changes could be associated with variability in the conditions in a nested-helical-field configuration is worthy of further study and may provide a relatively simple way to explain RM sign changes without invoking dramatic bending of the jet relative to the line of sight.

2.4. Inverse Depolarization

Looking at the wavelength dependence of the degree of polarization of a large sample of AGN in the range 8.1–15.4 GHz, Hovatta et al. [35] found that most of these sources displayed the decrease in their degree of polarization with decreasing frequency that is expected due to the action of Faraday and beamwidth depolarization. However, a small number of sources displayed the opposite tendency: increasing polarization with decreasing frequency, termed “inverse depolarization” by Homan [36]. Homan [36] presented a physical model for this phenomenon in which the structure of the jet magnetic field is such that internal Faraday rotation acts to align the polarization from the far and near sides of the jet; this leads to higher fractional polarization at longer wavelengths, where the superposed polarization from these two regions becomes better aligned. This effect can be produced naturally in both helical \mathbf{B} fields and randomly-tangled magnetic fields; however, in the latter case, the fields must be tangled on length scales in the jet that are too long to be consistent with the observed levels of fractional polarization, making helical jet \mathbf{B} fields a more attractive option. Homan [36] also notes that three of the four features that display inverse depolarization are in jets that have transverse RM gradients—a clear signature of the presence of a toroidal field that may represent one component of a helical field—increasing the likelihood that the explanation for this anomalous polarization behaviour lies in helical \mathbf{B} fields carried by these jets. Incidentally, this is an example of the role of “Occam’s razor” in helping us identify the simplest and most likely interpretation of the collected data.

2.5. Variability of Jet Ridge Lines

In their study of the kinematics of ridge lines of the VLBI jet of BL Lac, Cohen et al. [37] identified transverse patterns in the ridge lines, which moved superluminally downstream. They suggested that these patterns were analogous to waves on a whip. This behaviour led them to a model for the observed variability of the jet ridge lines in which the jet carries a tightly-wound helical \mathbf{B} field, and the transverse patterns represent Alfvén waves propagating downstream along the longitudinal component of this helical field.

2.6. Large Polarization Angle Rotations Associated with Outbursts

Marscher et al. [24] carried out detailed analyses of sequences of VLBI images together with optical polarization measurements of BL Lac in order to probe the acceleration and collimation region upstream of the observed VLBI core. They suggested that rapid, smooth rotations of the polarization could reflect the motion of a polarized region in the jet along a helical stream-line, such as those expected in the model of [23]. Their analysis showed that a bright feature in the VLBI jet caused a double flare observed from optical up to TeV energies, accompanied by rotation of the observed polarization angle and a delayed outburst at radio wavelengths. Marscher et al. [24] concluded that

this event was initiated in a region of helical **B** field, which they identified with the acceleration and collimation zone predicted theoretically, on scales upstream from the observed millimetre-VLBI core.

2.7. Double Polarization Angle Rotations

Cohen et al. [38] observed four double polarization angle rotations in OJ 287, in which the polarization angle rotated counter-clockwise for $\simeq 180^\circ$ and then rotated clockwise back to roughly its initial value, over an overall time of 1–3 years. They were able to explain this phenomenon with a model in which two successive polarized outbursts occur, with the polarization angles rotating in each, but in opposite directions, superposed on a constant polarization component corresponding to the underlying quiescent jet. The question then becomes how to explain the occurrence of such pairs of counter-rotating polarized outbursts: Cohen et al. [38] suggested that these can be generated by the supermagnetosonic jet model of Nakamura et al. [39] and Nakamura and Meier [40], in which the jet carries a strong helical magnetic field. The pairs of outbursts are associated with forward and reverse pairs of fast and slow magnetohydrodynamical waves; the plasma inside the two fast/slow pairs rotates in a helical pattern around the axis of the jet, but in opposite directions.

This study supports the earlier suggestion by Cohen [41] that the jet of OJ 287 carries a helical **B** field, based on the evolution of the jet ridge lines, which are twisted and can be interpreted as sections of a rotating helix, as in the model of [39,40].

2.8. Circular Polarization

The circular polarization of synchrotron radiation is intrinsically much less than 1%. At the same time, a substantial minority (about 15%) of radio-loud AGN display low, but significant levels of circular polarization, typically a few tenths of a percent [42]. Thus, some other mechanism is required to explain this, and it is generally believed that the best candidate is the Faraday conversion of linear to circular polarization in a magnetized plasma [43]. Faraday conversion can operate in any situation where a linearly-polarized electromagnetic wave propagates through a region of magnetized plasma with a non-zero component of the ambient magnetic field parallel to the electric field of the wave. Most importantly, Faraday conversion is more efficient at generating circular polarization than the synchrotron mechanism under similar conditions. The presence of a helical jet **B** field provides a natural configuration facilitating Faraday conversion: linearly-polarized radiation emitted at the far side of the jet relative to the observer can be partially converted to circularly-polarized emission as it passes through the part of the helical field that is at the near side of the jet ([44,45]). Thus, transverse RM gradients and circular polarization exceeding the level expected for the synchrotron mechanism are both signs of a helical jet **B** field. When these properties are both detected, they can be analysed together with the jet's linear polarization structure to determine uniquely the direction of the longitudinal component of the helical **B** field, and hence infer the direction of the rotation of the central black hole and its accretion disk. Such an analysis was recently carried out for 12 AGN by Gabuzda [46]. Her results indicate numbers of outward and inward longitudinal **B**-field components that are equal within the statistical uncertainties and also statistically equal numbers of central black holes rotating clockwise and counter-clockwise projected on the sky. At the same time, the results suggest that the directions of the longitudinal field and of the central rotation are coupled: clockwise central rotation projected onto the sky is preferentially associated with an inward longitudinal **B** field, while counter-clockwise rotation is associated with an outward longitudinal **B** field. Together, this gives rise to a preferred orientation for the toroidal component of the resulting helical **B** field, which corresponds to inward current along the jet axis on parsec scales, just as is predicted by the cosmic battery mechanism of [8,9].

3. Summary

AGN jets are expected theoretically to carry helical **B** fields, due to the joint action of the rotation of the central black hole and accretion disk and the jet outflow. There is now substantial observational

evidence that many or all jets do indeed carry helical **B** fields. The most direct evidence comes from the detection of statistically-significant transverse Faraday RM gradients across the jets of some 50 AGN on parsec scales and about a dozen AGN on larger scales of tens to thousands of parsecs. This clearly indicates that these helical fields persist to substantial distances from the jet base.

Furthermore, many of the characteristic polarization/magnetic-field structures observed in AGN jets on parsec scales can be understood as manifestations of a helical jet **B** field. Other evidence comes from studies of a wide variety of phenomena, including circular polarization, inverse depolarization, variability in jet ridge lines and the RM sign and polarization-angle rotations. There is considerable hope for building up links between these observations, since AGN jets carrying helical **B** fields may well display more than one of these phenomena, as well as polarization structures characteristic of helical jet **B** fields and transverse RM gradients. Joint analyses of the linear polarization structure, circular polarization sign and transverse RM gradients are a potentially powerful tools for revealing the full three-dimensional structures of helical **B** fields carried by AGN jets.

At the same time, some of the characteristic polarization structures observed in AGN jets are also consistent with the action of local agents, such as shocks, shear and jet bending. It can be difficult to identify unambiguously the origin of observed polarization structures in particular jets in practice without incorporating additional information about the distribution of the degree of polarisation, the morphology of the jet, the distribution of Faraday rotation in the vicinity of the jet and the possible presence of transverse RM gradients across the jet. In many cases, it is likely that the observed polarization structure is produced by both the intrinsic helical **B** field of the jet and the action of various local factors. One local factor that has been neglected so far in interpretations of observational data, but that may well play an important role, especially in variability, is magnetic reconnection. Work on identifying observational signatures of magnetic reconnection in AGN jets is needed.

The direction of a transverse RM gradient across an AGN jet implies a direction for the azimuthal **B**-field component producing it, which, in turn, implies the direction for the net current flowing inside the region occupied by this toroidal field. The collected data on transverse RM gradients observed on parsec to kiloparsec scales demonstrate a statistically-significant predominance of inward currents along the jet axis on parsec scales (probability of the predominance being spurious $\simeq 0.40\%$) and of outward currents on decaparsec–kiloparsec scales (probability of the predominance being spurious $\simeq 0.05\%$), presumably in a more extended region surrounding the jet. This is fully consistent with the nested-helical-field structure predicted by the “cosmic battery” model described in [8,9]. In this picture, the systems of currents and fields in AGN jets and their accretion disks are essentially similar to those for giant co-axial cables. Simulations of jet launching and propagation taking into account this type of nested-helical-field structure would be very valuable.

Thus, we are essentially in the process of initiating a new paradigm, in which the observed polarization (magnetic-field) structures in AGN jets on essentially all scales are at least partially due to the helical **B** fields carried by these jets. Superposed on the intrinsic polarization patterns associated with these helical fields are the results of local effects, such as shocks, shear, turbulence, jet bending, and magnetic reconnection. Although it may be virtually impossible to determine unambiguously precisely what factors are contributing to the observed polarization structure of a particular AGN jet, joint analyses of multiple types of observations provide hope for giving us some idea of how much of the observed patterns is due to the intrinsic helical jet **B** field and how much is associated with local effects. This will present interesting challenges for future studies in this area.

Funding: This research received no external funding.

Conflicts of Interest: The author declares no conflict of interest.

References

1. Kellermann, K.I.; Sramek, R.; Schmidt, M.; Shaffer, D.B.; Green, R. VLA observations of objects in the Palomar Bright Quasar Survey. *Astron. J.* **1989**, *98*, 1195–1207. [[CrossRef](#)]

2. Blandford, R.D.; Payne, D.G. Hydromagnetic Flows from Accretion Discs and the Production of Radio Jets. *Mon. Not. R. Astron. Soc.* **1982**, *199*, 883–903. [[CrossRef](#)]
3. Blandford, R.D.; Znajek, R.L. Electromagnetic Extraction of Energy from Kerr Black Holes. *Mon. Not. R. Astron. Soc.* **1977**, *179*, 433–456. [[CrossRef](#)]
4. Nakamura, M.; Uchida, Y.; Hirose, S. Production of Wiggled Structure of AGN Radio Jets in the Weeping Magnetic Twist Mechanism. *New Astron.* **2001**, *6*, 61–78. [[CrossRef](#)]
5. Lovelace, R.V.E.; Li, H.; Koldoba, A.V.; Ustyugova, G.V.; Romanova, M.M. Poynting Jets from Accretion Disks. *Astrophys. J.* **2002**, *572*, 445–455. [[CrossRef](#)]
6. Tchekhovskoy, A.; Bromberg, O. Three-dimensional Relativistic MHD Simulations of Active Galactic Nuclei Jets: Magnetic Kink Instability and Fanaroff-Riley Dichotomy. *Mon. Not. R. Astron. Soc.* **2016**, *461*, L46–L50. [[CrossRef](#)]
7. Barniol Duran, R.; Tchekhovskoy, A.; Giannios, D. Simulations of AGN Jets: Magnetic Kink Instability versus Conical Shocks. *Mon. Not. R. Astron. Soc.* **2017**, *469*, 4957–4978. [[CrossRef](#)]
8. Contopoulos, I.; Christodoulou, D.; Kazanas, D.; Gabuzda, D.C. The Invariant Twist of Magnetic Fields in the Relativistic Jets of Active Galactic Nuclei. *Astrophys. J.* **2009**, *702*, L148–L152. [[CrossRef](#)]
9. Christodoulou, D.; Gabuzda, D.; Knuettel, S.; Contopoulos, I.; Kazanas, D.; Coughlan, C. Dominance of Outflowing Electric Currents on Decaparsec to Kiloparsec Scales in Extragalactic Jets. *Astron. Astrophys.* **2016**, *591*, A61–A71.
10. Gabuzda, D.C.; Roche, N.; Kirwan, A.; Knuettel, S.; Nagle, M.; Houston, C. Parsec Scale Faraday-rotation Structure Across the Jets of Nine Active Galactic Nuclei. *Astron. Astrophys.* **2017**, *472*, 1792–1801.
11. Pacholczyk, A.G. *Radio Astrophysics*; W. H. Freeman: San Francisco, CA, USA, 1970.
12. Wardle, J.F.C. The Variable Rotation Measure Distribution in 3C 273 on Parsec Scales. *Galaxies* **2018**, *6*, 5. [[CrossRef](#)]
13. Blandford, R.D.; Königl, A. Relativistic Jets as Compact Radio Sources. *Astrophys. J.* **1979**, *232*, 34–48. [[CrossRef](#)]
14. Lister, M.L.; Homan, D.C. MOJAVE: Monitoring of Jets in Active Galactic Nuclei with VLBA Experiments. I. First-Epoch 15 GHz Linear Polarization Images. *Astron. J.* **2005**, *130*, 1389–1417. [[CrossRef](#)]
15. Gabuzda, D.C. Parsec-Scale Jets in Active Galactic Nuclei. In *The Formation and Disruption of Black Hole Jets*; Astrophysics and Space Science Library; Springer International: Cham, Switzerland, 2015; Volume 414, pp. 117–148.
16. Lyutikov, M.; Pariev, V.I.; Gabuzda, D.C. Polarization and Structure of Relativistic Parsec-scale AGN Jets. *Mon. Not. R. Astron. Soc.* **2005**, *360*, 869–891. [[CrossRef](#)]
17. Pushkarev, A.B.; Gabuzda, D.C.; Vetukhnovskaya, Y.N.; Yakimov, V.E. Spine-sheath Polarization Structures in Four Active Galactic Nuclei Jets. *Mon. Not. R. Astron. Soc.* **2005**, *356*, 859–871. [[CrossRef](#)]
18. Murphy, E.; Cawthorne, T.V.; Gabuzda, D.C. Analysing the Transverse Structure of the Relativistic Jets of Active Galactic Nuclei. *Mon. Not. R. Astron. Soc.* **2013**, *430*, 1504–1515. [[CrossRef](#)]
19. Hughes, P.A.; Aller, H.D.; Aller, M.A. iPolarized Radio Outbursts in BL Lacertae—Part Two—The Flux and Polarization of a Piston-Driven Shock. *Astrophys. J.* **1985**, *298*, 301–315. [[CrossRef](#)]
20. Hughes, P.A.; Aller, H.D.; Aller, M.A. Synchrotron Emission from Shocked Relativistic Jets. II. A Model for the Centimeter Wave Band Quiescent and Burst Emission from BL Lacertae. *Astrophys. J.* **1989**, *341*, 68–79. [[CrossRef](#)]
21. Laing, R. A Model for the Magnetic-field Structure in Extended Radio Sources. *Mon. Not. R. Astron. Soc.* **1980**, *193*, 439–449. [[CrossRef](#)]
22. Marscher, A.P.; Gear, W.K. Models for High-frequency Radio Outbursts in Extragalactic Sources, with Application to the early 1983 Millimeter-to-infrared Flare of 3C 273. *Astrophys. J.* **1985**, *298*, 114–127. [[CrossRef](#)]
23. Vlahakis, N. Disk-Jet Connection. In *Blazar Variability Workshop II: Entering the GLAST Era*; Astronomical Society of the Pacific: San Francisco, CA, USA, 2006; Volume 350, pp. 169–177.
24. Marscher, A.P.; Jorstad, S.G.; D’Arcangelo, F.D.; Smith, P.S.; Williams, G.G.; Larionov, V.M.; Oh, H.; Olmstead, A.R.; Aller, M.F.; Aller, H.D.; et al. The Inner Jet of an Active Galactic Nucleus as Revealed by a Radio-to- γ -ray Outburst. *Nature* **2008**, *452*, 966–969. [[CrossRef](#)] [[PubMed](#)]

25. Lobanov, A.; Hardee, P.; Eilek, J. Double Helix in the Kiloparsec-Scale Jet in M 87. In *Future Directions in High Resolution Astronomy: The 10th Anniversary of the VLBA*; Astronomical Society of the Pacific: San Francisco, CA, USA, 2005; Volume 340, pp. 104–106.
26. Lobanov, A.P.; Zensus, J.A. A Cosmic Double Helix in the Archetypical Quasar 3C273. *Science* **2001**, *294*, 128–131. [[CrossRef](#)] [[PubMed](#)]
27. Blandford, R.D. *Astrophysical Jets*; Cambridge University Press: Cambridge, UK, 1993; p. 26.
28. Perley, R.A.; Bridle, A.H.; Willis, A.G. High-resolution VLA Observations of the Radio Jet in NGC 6251. *Astrophys. J. Suppl.* **1984**, *54*, 291–334. [[CrossRef](#)]
29. Asada, K.; Inoue, M.; Uchida, Y.; Kamenno, S.; Fujisawa, K.; Iguchi, S.; Mutoh, M. A Helical Magnetic Field in the Jet of 3C 273. *Publ. Astron. Soc. Jpn.* **2002**, *54*, L39–L43. [[CrossRef](#)]
30. Gabuzda, D.C.; Nagle, M.; Roche, N. The Jets of AGN as Giant Coaxial Cables. *Astron. Astrophys.* **2018**, *612*, A67–A79.
31. Knuettel, S.; Gabuzda, D.C.; O’Sullivan, S.P. Evidence for Toroidal B-Field Components in AGN Jets on Kiloparsec Scales. *Galaxies* **2017**, *5*, 61. [[CrossRef](#)]
32. Mahmud, M.; Coughlan, C.P.; Murphy, E.; Gabuzda, D.C.; Hallahan, D.R. Connecting Magnetic Towers with Faraday Rotation Gradients in Active Galactic Nuclei Jets. *Mon. Not. R. Astron. Soc.* **2013**, *431*, 695–709. [[CrossRef](#)]
33. Koutsantoniou, L.; Contopoulos, I. Accretion Disk Radiation Dynamics and the Cosmic Battery. *Astrophys. J.* **2014**, *794*, 27–38. [[CrossRef](#)]
34. Lico, R.; Gomez, J.L.; Asada, K.; Fuentes, A. On the Time Variable Rotation Measure in the Core Region of Markarian 421. *Galaxies* **2017**, *5*, 57. [[CrossRef](#)]
35. Hovatta, T.; Lister, M.L.; Aller, M.F.; Aller, H.D.; Homan, D.C.; Kovalev, Y.Y.; Pushkarev, A.B.; Savolainen, T. MOJAVE: Monitoring of Jets in Active Galactic Nuclei with VLBA Experiments. VIII. Faraday Rotation in Parsec-scale AGN Jets. *Astron. J.* **2012**, *144*, 105–138. [[CrossRef](#)]
36. Homan, D.C. Inverse Depolarization: A Potential Probe of Internal Faraday Rotation and Helical Magnetic Fields in Extragalactic Radio Jets. *Astrophys. J.* **2012**, *757*, L24–L28. [[CrossRef](#)]
37. Cohen, M.H.; Meier, D.L.; Arshakian, T.G.; Clausen-Brown, E.; Homan, D.C.; Hovatta, T.; Kovalev, Y.Y.; Lister, M.L.; Pushkarev, A.B.; Richards, J.L.; et al. Studies of the Jet in Bl Lacertae. II. Superluminal Alfvén Waves. *Astrophys. J.* **2015**, *803*, 3. [[CrossRef](#)]
38. Cohen, M.H.; Aller, H.D.; Aller, M.F.; Hovatta, T.; Kharb, P.; Kovalev, Y.Y.; Lister, M.L.; Meier, D.L.; Pushkarev, A.B.; Savolainen, T. Reversals in the Direction of Polarization Rotation in OJ 287. *Astrophys. J.* **2018**, *862*, 1. [[CrossRef](#)]
39. Nakamura, M.; Garofalo, D.; Meier, D.L. A Magnetohydrodynamic Model of the M87 Jet. I. Superluminal Knot Ejections from HST-1 as Trails of Quad Relativistic MHD Shocks. *Astrophys. J.* **2010**, *721*, 1783–1789. [[CrossRef](#)]
40. Nakamura, M.; Meier, D.L. A Magnetohydrodynamic Model of the M87 Jet. II. Self-consistent Quad-shock Jet Model for Optical Relativistic Motions and Particle Acceleration. *Astrophys. J.* **2014**, *785*, 152–157. [[CrossRef](#)]
41. Cohen, M.H. OJ 287 as a Rotating Helix. *Galaxies* **2017**, *5*, 12. [[CrossRef](#)]
42. Homan, D.C.; Lister, M.L. iMOJAVE: Monitoring of Jets in Active Galactic Nuclei with VLBA Experiments. II. First-Epoch 15 GHz Circular Polarization Results. *Astron. J.* **2006**, *131*, 1262–1279. [[CrossRef](#)]
43. Jones, T.W.; O’Dell, S.L. Transfer of Polarized Radiation in Self-absorbed Synchrotron Sources. I. Results for a Homogeneous Source. *Astrophys. J.* **1977**, *214*, 522–539. [[CrossRef](#)]
44. Ensslin, T.A. Does Circular Polarisation Reveal the Rotation of Quasar Engines? *Astron. Astrophys.* **2003**, *401*, 499–504.
45. Wardle, J.F.C.; Homan, D.A. The Nature of Jets: Evidence from Circular Polarization Observations. In *Particles and Fields in Radio Galaxies*; Astronomical Society of the Pacific: San Francisco, CA, USA, 2001; pp. 152–163.
46. Gabuzda, D.C. Determining the Jet Poloidal B Field and Black-Hole Rotation Directions in AGNs. *Galaxies* **2018**, *6*, 9. [[CrossRef](#)]

